nature geoscience

ARTICLES

PUBLISHED ONLINE: 8 FEBRUARY 2016 | DOI: 10.1038/NGEO2657

Sequestration of carbon in the deep Atlantic during the last glaciation

J. Yu[1]*, L. Menviel[2,3], Z. D. Jin[4], D. J. R. Thornalley[5], S. Barker[6], G. Marino[1], E. J. Rohling[1,7], Y. Cai[4], F. Zhang[4], X. Wang[8], Y. Dai[1], P. Chen[1,9] and W. S. Broecker[10]

Atmospheric CO_2 concentrations declined markedly about 70,000 years ago, when the Earth's climate descended into the last glaciation. Much of the carbon removed from the atmosphere has been suspected to have entered the deep oceans, but evidence for increased carbon storage remains elusive. Here we use the B/Ca ratios of benthic foraminifera from several sites across the Atlantic Ocean to reconstruct changes in the carbonate ion concentration and hence the carbon inventory of the deep Atlantic across this transition. We find that deep Atlantic carbonate ion concentration declined by around 25 μmol kg^{-1} between ~80,000 and 65,000 years ago. This drop implies that the deep Atlantic carbon inventory increased by at least 50 Gt around the same time as the amount of atmospheric carbon dropped by about 60 Gt. From a comparison with proxy records of deep circulation and climate model simulations, we infer that the carbon sequestration coincided with a shoaling of the Atlantic meridional overturning circulation. We thus conclude that changes in the Atlantic Ocean circulation may have played an important role in reductions of atmospheric CO_2 concentrations during the last glaciation, by increasing the carbon storage in the deep Atlantic.

Ice-core records show a tight correlation between changes in atmospheric CO_2 and Antarctic temperature, suggesting an important impact of atmospheric CO_2 fluctuations on Earth's climate on orbital and millennial timescales[1,2]. During the last glacial cycle, a major climate change occurred at the Marine Isotope Stage (MIS) 5–4 transition around 70 thousand years ago (ka), with significant global cooling, substantial build-up of polar ice sheets, and profound ocean circulation changes[2–6]. The atmospheric CO_2 decline across this transition accounts for about one-third of the entire interglacial–glacial atmospheric CO_2 drawdown[1,2]. Although the deep ocean is the widely suspected culprit for lowering glacial atmospheric CO_2 (refs 7,8), through biogeochemical and physical processes[5,9–11], convincing evidence for carbon sequestration in the deep ocean is limited[12,13], and the role of ocean circulation changes in deep-sea carbon storage remains elusive[5,9]. Here, we quantify carbon budget change in the deep Atlantic and investigate its relationship with changes in the Atlantic meridional ocean circulation (AMOC) across the MIS 5–4 transition.

Seawater carbonate ion concentration ($[CO_3^{2-}]$) is primarily governed by dissolved inorganic carbon (DIC) and alkalinity (ALK; Fig. 1); other parameters such as temperature and salinity play only minor roles when ALK and DIC remain unchanged[14,15]. Changes (Δ) in $[CO_3^{2-}]$, DIC and ALK can be approximated by

$$\Delta_{[CO_3^{2-}]} \approx k \times (\Delta_{ALK} - \Delta_{DIC}) \quad (1)$$

where $k = 0.59 \pm 0.01$ (1σ; used throughout; Supplementary Figs 1 and 2). Therefore, with sound knowledge about Δ_{ALK}, reconstructions of deep-water $\Delta_{[CO_3^{2-}]}$ allow an estimate of Δ_{DIC}, the term that ultimately determines the carbon budget change of the investigated ocean reservoir. Equation (1) successfully predicts DIC in the pre-industrial deep Atlantic Ocean[16] (Fig. 1b).

Deep Atlantic $[CO_3^{2-}]$ reconstructions

We present deep-water $[CO_3^{2-}]$ during ~90–50 ka for 10 sediment cores (6 new and 4 from refs 17,18) from a wide geographic and depth range in the Atlantic Ocean (Fig. 1). Deep-water $[CO_3^{2-}]$ is reconstructed using B/Ca in the epifaunal benthic foraminifer *Cibicidoides wuellerstorfi*, with an uncertainty of ±5 μmol kg^{-1} for $[CO_3^{2-}]$ from core-top calibration[19] (Supplementary Fig. 3). Sediment-core age models are constructed by tuning all benthic $\delta^{18}O$ records to the LR04 $\delta^{18}O$ stack[20](Supplementary Figs 4–6 and Supplementary Tables 1–3). The age ranges for MIS 5a (85–75 ka) and MIS 4 (69–59 ka) are based on light (≲3.3‰) and heavy (≳3.8‰) benthic $\delta^{18}O$ values, respectively.

Figure 2 shows that *C. wuellerstorfi* B/Ca decreased from MIS 5a to MIS 4 in all 10 cores. Relative to mean MIS 5a, deviations of B/Ca ($\Delta_{B/Ca}$) during MIS 4 are -20 ± 5 μmol mol^{-1} ($n = 35$) in 7 cores from the eastern basin and -42 ± 11 μmol mol^{-1} ($n = 21$) in 3 cores (EW9209-2JPC, RC16-59, and GeoB1118-3) from the western Atlantic (Fig. 3a,b and Supplementary Table 4). As *C. wuellerstorfi* B/Ca is minimally biased by post-mortem dissolution[19,21], we attribute decreased MIS 4 B/Ca values to reductions in deep-water $[CO_3^{2-}]$. Using a core-top-derived sensitivity of 1.14 μmol mol^{-1} per μmol kg^{-1} specific to *C. wuellerstorfi*[19], benthic $\Delta_{B/Ca}$ values suggest 18 ± 6 and

[1]Research School of Earth Sciences, The Australian National University, Canberra, Australian Capital Territory 2601, Australia. [2]Climate Change Research Centre, University of New South Wales, New South Wales 2052, Australia. [3]ARC Centre of Excellence for Climate System, New South Wales 2052, Australia. [4]State Key Laboratory of Loess and Quaternary Geology, Institute of Earth Environment, Chinese Academy of Sciences, Xi'an 710075, China. [5]Department of Geography, University College London, London WC1E 6BT, UK. [6]School of Earth and Ocean Sciences, Cardiff University, Cardiff CF10 3XQ, UK. [7]Ocean and Earth Science, University of Southampton, National Oceanography Centre, Southampton SO14 3ZH, UK. [8]Earth Observatory of Singapore, Nanyang Technological University, 50 Nanyang Avenue, 639798, Singapore. [9]School of Geographic Sciences, East China Normal University, Shanghai 200241, China. [10]Lamont-Doherty Earth Observatory of Columbia University, 61 Route 9W/PO Box 1000, Palisades, New York 10964-8000, USA. *e-mail: jimin.yu@anu.edu.au

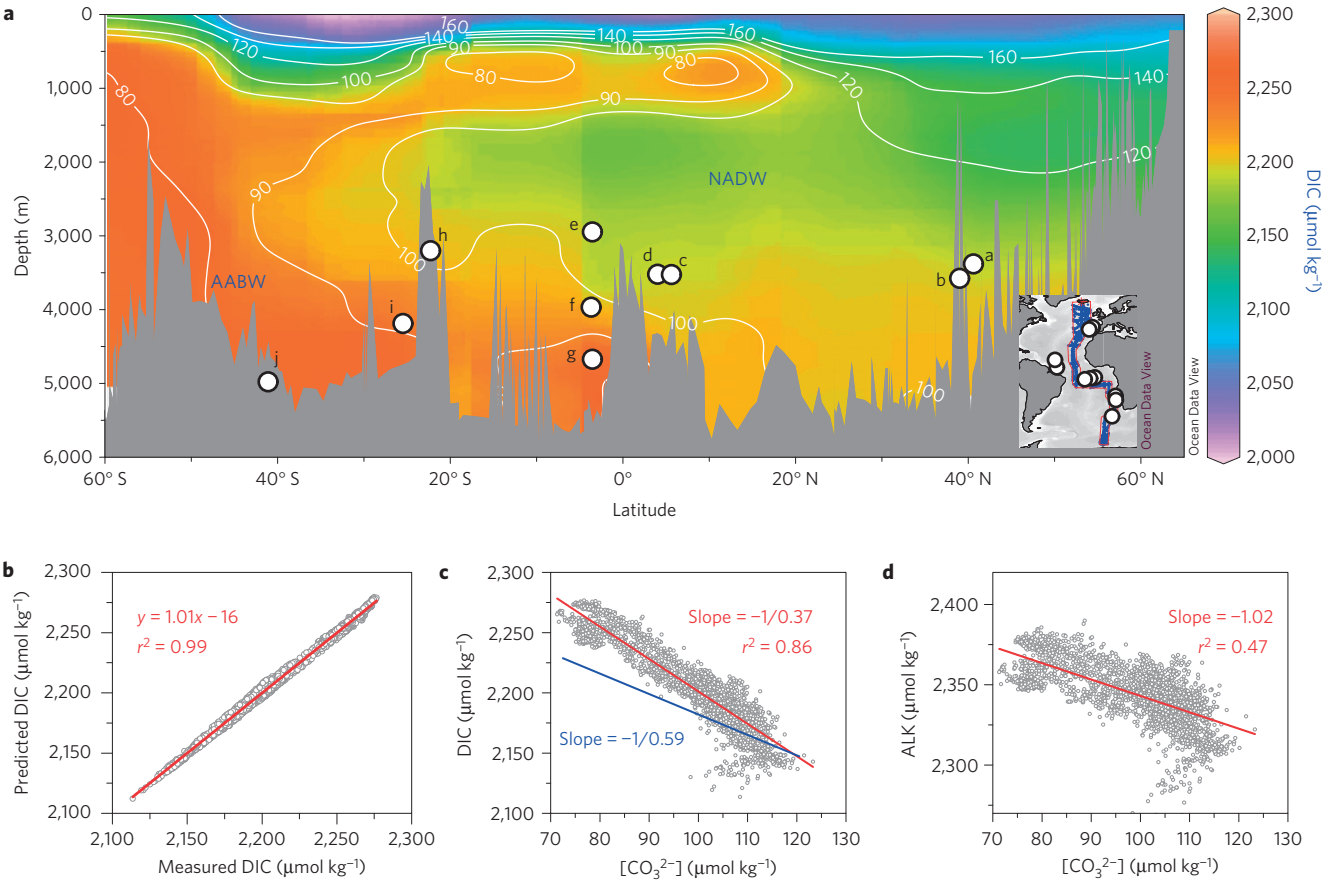

Figure 1 | Pre-industrial Atlantic Ocean carbonate chemistry and sediment cores. a, Locations of studied cores (circles) against meridional DIC (colour-shading) and $[CO_3^{2-}]$ (contours, μmol kg^{-1}). Inset shows the transect[16,47]. Cores: a, MD95-2039; b, MD01-2446; c, EW9209-2JPC; d, RC16-59; e, GEOB1115-3; f, GEOB1117-2; g, GEOB1118-3; h, RC13-228; i, RC13-229; j, TNO57-21 (Supplementary Table 1). **b**, Predicted versus measured DIC. **c**, DIC versus $[CO_3^{2-}]$. The blue line shows the expected DIC trend based on equation (1) when $\Delta_{ALK} = 0$ (Supplementary Information). **d**, ALK versus $[CO_3^{2-}]$. Red lines (**b**–**d**) represent linear regressions of the deep Atlantic data (>2.5 km, 70° S–70° N, 15° E–65° W; ref. 16).

37 ± 12 μmol kg^{-1} $[CO_3^{2-}]$ reductions in the eastern and western basins, respectively (Fig. 3a). Considering all 10 cores, benthic B/Ca decreased by 28 ± 13 μmol mol^{-1} ($n = 56$), corresponding to a 25 ± 13 μmol kg^{-1} decline in $[CO_3^{2-}]$, from MIS 5a to MIS 4 (Fig. 3).

Different from $\Delta_{B/Ca}$, benthic $\delta^{13}C$ amplitudes are similar between cores at ~3.5 km water depth from the eastern (MD01-2446 and MD95-2039) and western (EW9209-2JPC and RC16-59) North Atlantic (Supplementary Fig. 7). One possibility for this contrast is different $\delta^{13}C$ endmembers in the source waters ventilating the two basins during MIS 4. $\delta^{13}C$ heterogeneity of northern-sourced waters has been reported for the Last Glacial Maximum[14,22]. We here attribute the larger $\Delta_{B/Ca}$ to a greater ocean circulation change in the western basin (Supplementary Fig. 8), necessitating a higher source-water $\delta^{13}C$ for the western Atlantic during MIS 4. Future work is required to validate this, but the associated uncertainties do not affect our conclusions.

Benthic B/Ca and $\delta^{18}O$ are negatively correlated in each core (Supplementary Figs 9 and 10). This suggests that the decrease in deep-water $[CO_3^{2-}]$ into MIS 4 was associated with deep-sea cooling and continental ice build-up, which are thought to be linked to declining atmospheric CO_2 during glaciation[1–3,23]. The overall pattern of deep-water $[CO_3^{2-}]$ changes, identified through Monte Carlo-style probabilistic assessment of the combined $[CO_3^{2-}]$ reconstructions for our 10 cores, shows a first-order similarity to the evolution of atmospheric CO_2, in that both deep Atlantic $[CO_3^{2-}]$ and atmospheric CO_2 decreased from MIS 5a to MIS 4 (Fig. 3c,d)[1,2]. This provides evidence to support previous suggestions[11,14,18,24] that changes in deep Atlantic carbonate chemistry played an important role in glacial–interglacial atmospheric CO_2 variations.

As our data are from 10 sites widely distributed in the Atlantic (water depth: ~2.9–5 km, latitude: 41° S–41° N; Fig. 1), we consider that the 25 ± 13 μmol kg^{-1} reduction in deep-water $[CO_3^{2-}]$ approximates the mean $[CO_3^{2-}]$ change in the entire deep Atlantic (≳3 km) from MIS 5a to 4 (Fig. 3a–c). As a cross-check, we use the $[CO_3^{2-}]$–$\delta^{13}C$ relationship and the mean deep Atlantic $\delta^{13}C$ change to infer the mean deep Atlantic $[CO_3^{2-}]$ decrease across the MIS 5a–4 transition (Supplementary Figs 11 and 12). In our 10 cores, deep-water $[CO_3^{2-}]$ is significantly correlated with benthic $\delta^{13}C$ ($r^2 = 0.50$, $P < 0.0001$), yielding a slope of 0.0228‰ per μmol kg^{-1}. A previous compilation study has revealed an average decline of ~0.45‰ in benthic $\delta^{13}C$ throughout the deep Atlantic from MIS 5a to MIS 4 (ref. 25). If the $[CO_3^{2-}]$–$\delta^{13}C$ relationship observed at our 10 geographically widely distributed sites is applicable to other locations in the deep Atlantic, a 0.45‰ drop in $\delta^{13}C$ suggests a ~20 μmol kg^{-1} reduction in deep-water $[CO_3^{2-}]$, falling within the uncertainty of 25 ± 13 μmol kg^{-1} calculated from our $[CO_3^{2-}]$ reconstructions (Fig. 3a–c).

Quantifying carbon sequestration

Equation (1) indicates that changes in $[CO_3^{2-}]$ depend on variations in ALK and DIC. Four lines of evidence suggest that the lowered deep-water $[CO_3^{2-}]$ during MIS 4 was not caused by an ALK drop, but by an increase in deep Atlantic DIC. First, when $[CO_3^{2-}]$

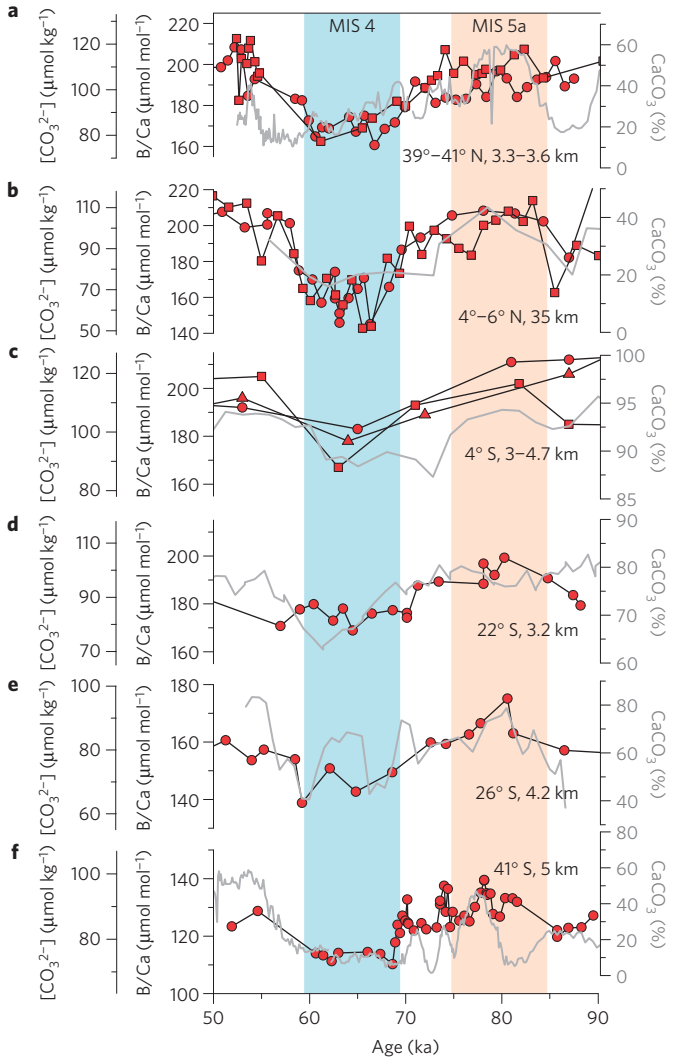

Figure 2 | Reconstructed $[CO_3^{2-}]$ from *C. wuellerstorfi* B/Ca in the deep Atlantic (≳3 km) during 90–50 ka. a, MD95-2039 (square) and MD01-2446 (circle). **b**, EW9209-2JPC (square) and RC16-59 (circle) (ref. 17 and this study). **c**, GeoB1115-3 (circle)[18], GeoB1117-2 (triangle)[18] and GeoB1118-3 (square)[18]. B/Ca data from GeoB1115-3 and GeoB1118-3 are shifted by −20 and +40 μmol mol^{-1}, respectively, to facilitate plotting. The $[CO_3^{2-}]$ scale is only for core GeoB1117-2. **d**, RC13-228. **e**, RC13-229. **f**, TNO57-21. Unless mentioned otherwise, B/Ca are from this study. Grey lines represent sediment carbonate contents (%$CaCO_3$). Shadings show MIS 5a (orange) and MIS 4 (cyan).

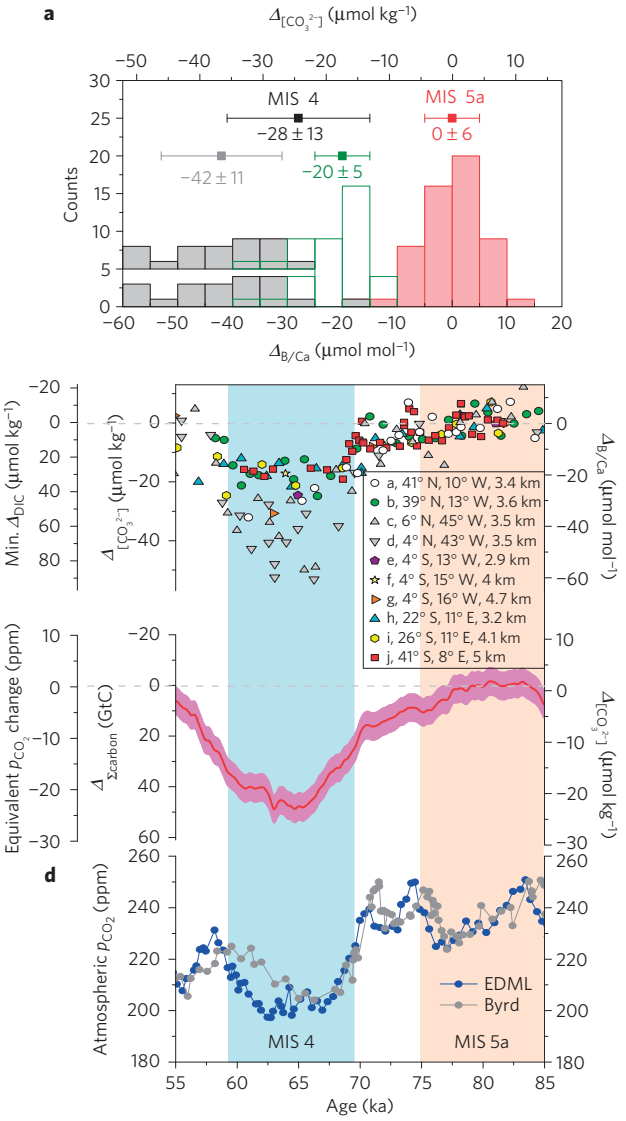

Figure 3 | Deep Atlantic carbon budget across the MIS 5a–4 transition. a, Histogram and averages (squares ±1 s.d.) of $\Delta_{B/Ca}$ (deviations of individual measurements from the B/Ca_{MIS5a} mean) and corresponding $\Delta_{[CO_3^{2-}]}$ (upper *x* axis) for MIS 5a (red) and 4 (green: eastern basin; grey: western basin; black: all cores). **b**, Temporal $\Delta_{B/Ca}$ and $\Delta_{[CO_3^{2-}]}$ evolutions, with minimum Δ_{DIC} calculated by equation (1) assuming $\Delta_{ALK} = 0$. Letters refer to cores, as shown in Fig. 1a. **c**, Monte Carlo-style probabilistic assessment of $[CO_3^{2-}]$ shown in **b** (curve: probability maximum; envelope: ±95% probability interval). $\Delta_{\Sigma carbon}$ represents minimum total carbon change in the deep Atlantic; its equivalent quantity in atmospheric CO_2 change is scaled by 1 ppm $CO_2 = 2.1$ GtC. **d**, Atmospheric CO_2 (refs 1,2). EDML, EPICA Dronning Maud Land; Byrd, Byrd Station, Antarctica.

declines, deep water becomes more corrosive and that would enhance water-column and deep-sea $CaCO_3$ dissolution, a process that drives up oceanic ALK (refs 8,14). This was illustrated in the pre-industrial Atlantic, where the $[CO_3^{2-}]$ decrease from North Atlantic Deep Water (NADW) to Antarctic Bottom Water (AABW) was accompanied by an ALK rise[16] (Fig. 1d). Our studied cores (Fig. 2) and many other locations in the deep Indo-Pacific[26–28] show intensified deep-sea $CaCO_3$ dissolution during the MIS 5a–4 transition, with a likely effect of raising the global oceanic ALK inventory[8,14]. Second, the ~50 m sea level drop into MIS 4 (ref. 3) would have substantially reduced the shelf area for neritic carbonate deposition, which in turn would have raised oceanic ALK (ref. 29). Third, benthic Ba/Ca ratios, a proxy for deep-water ALK (ref. 30), show some sign of increase during MIS 4 at four locations in the Atlantic (Supplementary Fig. 13). Fourth, model studies suggest higher ocean ALK in glacials than in interglacials[11,31].

To quantify the magnitude of deep-water DIC increase (Fig. 3b and Supplementary Information), we first assume no change in ALK (that is, $\Delta_{ALK} = 0$), and subsequently evaluate how this assumption affects the conclusions. According to equation (1), a 25 ± 13 μmol kg^{-1} decline in deep-water $[CO_3^{2-}]$ translates into a 42 ± 22 μmol kg^{-1} increase in DIC. Using a mass of 10.1×10^{19} kg for waters below 3 km in the Atlantic, we calculate that a total amount of 51 ± 27 Gt extra carbon was sequestered in the deep Atlantic during the MIS 5a–4 transition (Fig. 3c). During this period, atmospheric CO_2 declined by 28 ± 11 ppm (MIS 5a: 237 ± 8 ppm; MIS 4: 208 ± 8 ppm), corresponding to a loss of 60 ± 23 Gt carbon from the atmosphere[1,2] (Fig. 3d). Therefore, the

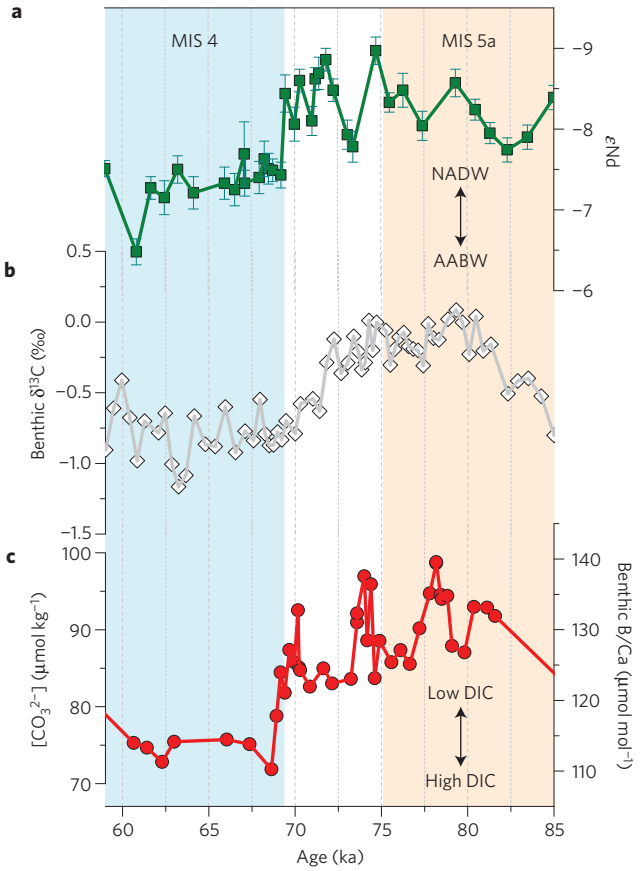

Figure 4 | Temporal evolution of geochemical proxies in core TNO57-21 from the deep South Atlantic. a, Sediment εNd, an ocean circulation proxy[9]. Error bars represent $\pm 1\sigma$ uncertainty. **b**, Benthic $\delta^{13}C$ (ref. 41), a geochemical tracer influenced by a combination of processes including ocean circulation, biogenic remineralization, and air–sea exchange, not all of which are associated with a change in deep-water DIC. **c**, Benthic B/Ca (this study), a proxy for deep-water $[CO_3^{2-}]$ that reflects changes in DIC and ALK, both of which are tightly linked to the carbon cycle in the ocean. The high sedimentation rate (~15 cm per 1,000 yr) in TNO57-21 through the 75–65 ka interval significantly minimizes bioturbation influences on geochemical tracers.

carbon stock increase in the deep Atlantic is, in quantity, equivalent to $\sim 86 \pm 56\%$ of the concurrent atmospheric CO_2 drawdown across the MIS 5a–4 transition.

Note that the deep Atlantic carbon budget change calculated above is likely to represent a conservative estimate owing to a possible rise in the global ocean ALK. CO_2 sequestration in the deep ocean across MIS 5a–4 would inevitably raise deep-water acidity, lower seawater $[CO_3^{2-}]$, and consequently intensify deep-sea $CaCO_3$ dissolution (Fig. 2). By raising the whole-ocean ALK, the so-called deep-sea carbonate compensation (Supplementary Information) serves as a negative feedback to restore the global deep-water $[CO_3^{2-}]$ to levels at which the global ocean ALK input (mainly from continental weathering) reaches a new steady state with ALK output (by shelf and deep-sea carbonate burial)[8,14,21,32–34]. The effect of carbonate compensation may be manifested by partial reversals of $[CO_3^{2-}]$ in MD01-2446, EW9209-2JPC and RC16-59 (Fig. 2). However, none of the studied $[CO_3^{2-}]$ records returned to the MIS 5a levels within the ~10,000-year duration of MIS 4, compared with the relaxation timescale of ~5–7,000 years associated with carbonate compensation[32]. Nevertheless, the deep Atlantic $[CO_3^{2-}]$ results shown in Fig. 3b cannot be treated as the global mean changes, for which $[CO_3^{2-}]$ variations in the deep Indo-Pacific have to be taken into account[33]. Considering the increased $CaCO_3$ burial and $[CO_3^{2-}]$ in the deep Pacific during the last phase of MIS 4 (refs 35,36), the steady-state global mean deep-water $[CO_3^{2-}]$ might remain roughly stable from MIS 5a to MIS 4, consistent with previous modelling work[33,37]. As there was increased carbon sequestration in the glacial deep ocean[7,8,11,12], a relatively stable deep-sea $[CO_3^{2-}]$ would suggest a greater ALK inventory during MIS 4. Alternatively, reduced weathering (perhaps induced by cold–dry glacial climates[32]) coupled with a weakening or shutdown of NADW can also maintain deep Atlantic $[CO_3^{2-}]$ at low values for ~8,000 years without invoking a global ALK change, as shown by models (Supplementary Figs 15 and 19). These scenarios are not mutually exclusive and are both consistent with the carbonate compensation theory. Insufficient evidence is available to reject either scenario, but a large change in weathering may not be expected given an opposing effect from the exposure of shelves[3] that tends to enhance carbonate weathering[38]. If global weathering remained roughly constant, then the global ocean ALK would have been higher during MIS 4 than during MIS 5a. Without a global ALK increase due to carbonate compensation, a much larger $[CO_3^{2-}]$ decrease would be expected in the deep Atlantic during MIS 4.

Given a deep-water $[CO_3^{2-}]$ reduction, equation (1) suggests that for every unit increase in ALK the DIC increase would be one unit higher than the number calculated assuming $\Delta_{ALK} = 0$. This is demonstrated by distributions of carbon species in today's Atlantic Ocean[16] (Fig. 1): to account for the ~40 μmol kg^{-1} $[CO_3^{2-}]$ reduction between NADW ($[CO_3^{2-}] = \sim 120$ μmol kg^{-1}) and AABW ($[CO_3^{2-}] = \sim 80$ μmol kg^{-1}), equation (1) would predict a $\Delta DIC_{AABW-NADW}$ of ~68 μmol kg^{-1} without any change in ALK, which is ~38% smaller than the observed DIC change (Fig. 1c). The difference is caused by a ~40 μmol kg^{-1} ALK increase from NADW to AABW (Fig. 1d). Had the pre-industrial $\Delta_{[CO_3^{2-}]}/\Delta_{DIC}$ ratio of −0.37 been applied, which empirically includes the ALK changes (Fig. 1c), then our calculated deep Atlantic carbon storage increase would be amplified by a factor of 1.6, and the quantity of carbon sequestration in the deep Atlantic would be comparable (within uncertainties) to the entire atmospheric CO_2 decline from MIS 5a to MIS 4. Additionally, consideration of larger $\Delta_{B/Ca}$ in the western Atlantic, which is under-sampled at present (Fig. 3a), would potentially raise the estimate of carbon sequestration in the deep Atlantic.

Reasons for carbon sequestration

Enhanced carbon storage in the deep Atlantic during MIS 4 may have resulted from a synergy of physical and biogeochemical processes[8,11]. Regarding physical processes, sediment neodymium isotopes (εNd; an ocean circulation proxy) imply an increased contribution of CO_2-rich southern-sourced abyssal waters (Fig. 1) in the deep Atlantic at the MIS 5a–4 transition[9,39]. During MIS 4, the NADW–AABW boundary probably shoaled to ~2–3 km water depth, and was located above major topographic ridges and seamounts[5,39]. Such an AMOC rearrangement would weaken diapycnal mixing between water masses, enhance water-column stratification, and thereby facilitate the retention of sequestered carbon in the deep ocean[4,40]. In core TNO57-21, a sharp ~1ε unit increase in εNd at ~70 ka (ref. 9) exactly coincided with a rapid ~12 μmol kg^{-1} decline in deep-water $[CO_3^{2-}]$ (Fig. 4). As seawater $[CO_3^{2-}]$ is primarily determined by DIC and ALK, both of which place direct constraints on the oceanic carbon cycle[8,11,32,34], synchronous changes in εNd and $[CO_3^{2-}]$ indicate a tight coupling between AMOC and carbon cycling in the deep Atlantic during the last glaciation. An ~0.5‰ decrease in benthic $\delta^{13}C$ (Fig. 4b)[41] at ~72 ka was previously interpreted to reflect a global carbon budget change to predate an AMOC reorganization[9]. Were this $\delta^{13}C$ decline caused by carbon transfer from land biosphere[9], it would concomitantly decrease deep-water $[CO_3^{2-}]$ and intensify deep-sea $CaCO_3$ dissolution, a phenomenon not observed in

TNO57-21 (Figs 2f and 4). Instead, we contend that the $\delta^{13}C$ decline might reflect processes such as air–sea isotopic exchange[42]. The coupling of AMOC and carbon cycling is further corroborated by results from two Earth system models of intermediate complexity: halving NADW formation leads to 10–30 µmol kg^{-1} reductions in [CO_3^{2-}] below ~3 km in the deep Atlantic without causing deep-sea anoxia (Supplementary Figs 22 and 23). Additionally, cooler climate during MIS 4 would raise CO_2 solubility and preformed DIC of deep waters[13,43], enhancing CO_2 sequestration in the deep ocean. Regarding the biogeochemistry, the decreased deep Atlantic [CO_3^{2-}] during MIS 4 is consistent with greater water-column remineralization due to reduced vertical mixing associated with a shoaled AMOC (refs 5,6,39,44) and a more efficient biological pump in the glacial Southern Ocean perhaps stimulated by increased iron availability[10], both of which would increase sequestration of respiratory DIC into the ocean interior and decrease atmospheric CO_2 (refs 8,11,45,46; Supplementary Fig. 25).

Overall, our calculations highlight that, despite its relatively modest proportion (~30%) of the global deep ocean volume, the deep Atlantic sequestered a substantial amount of carbon during the last glaciation at ~70 ka. The sequestered amount is quantitatively comparable to the contemporary carbon loss from the atmosphere. We also find that this large carbon sequestration was tightly coupled with AMOC changes. The movements of carbon between reservoirs in the atmosphere–land biosphere–ocean system are intricately linked, and future studies may aim to quantify the contributions from individual sources to the increased carbon storage in the deep ocean during glaciations.

Methods

Methods and any associated references are available in the online version of the paper.

Received 10 September 2015; accepted 14 January 2016; published online 8 February 2016

References

1. Ahn, J. & Brook, E. J. Atmospheric CO_2 and climate on millennial time scales during the last glacial period. *Science* **322**, 83–85 (2008).
2. Bereiter, B. *et al*. Mode change of millennial CO_2 variability during the last glacial cycle associated with a bipolar marine carbon seesaw. *Proc. Natl Acad. Sci. USA* **109**, 9755–9760 (2012).
3. Grant, K. M. *et al*. Rapid coupling between ice volume and polar temperature over the past 150,000 years. *Nature* **491**, 744–747 (2012).
4. Adkins, J. F. The role of deep ocean circulation in setting glacial climates. *Paleoceanography* **28**, 539–561 (2013).
5. Thornalley, D. J. R., Barker, S., Becker, J., Hall, I. R. & Knorr, G. Abrupt changes in deep Atlantic circulation during the transition to full glacial conditions. *Paleoceanography* **28**, 253–262 (2013).
6. Barker, S. & Diz, P. Timing of the descent into the last ice age determined by the bipolar seesaw. *Paleoceanography* **29**, 489–507 (2014).
7. Broecker, W. Glacial to interglacial changes in ocean chemistry. *Prog. Oceanogr.* **2**, 151–197 (1982).
8. Sigman, D. M. & Boyle, E. A. Glacial/interglacial variations in atmospheric carbon dioxide. *Nature* **407**, 859–869 (2000).
9. Piotrowski, A., Goldstein, S. J., Hemming, S. R. & Fairbanks, R. G. Temporal relationships of carbon cycling and ocean circulation at glacial boundaries. *Science* **307**, 1933–1938 (2005).
10. Martinez-Garcia, A. *et al*. Iron fertilization of the subantarctic ocean during the last ice age. *Science* **343**, 1347–1350 (2014).
11. Hain, M. P., Sigman, D. M. & Haug, G. H. Carbon dioxide effects of Antarctic stratification, North Atlantic Intermediate Water formation, and subantarctic nutrient drawdown during the last ice age: diagnosis and synthesis in a geochemical box model. *Glob. Biogeochem. Cycles* **24**, GB4023 (2010).
12. Hoogakker, B. A. A., Elderfield, H., Schmiedl, G., McCave, I. N. & Rickaby, R. E. M. Glacial–interglacial changes in bottom-water oxygen content on the Portuguese margin. *Nature Geosci.* **8**, 40–43 (2015).
13. Goodwin, P. & Lauderdale, J. M. Carbonate ion concentrations, ocean carbon storage, and atmospheric CO_2. *Glob. Biogeochem. Cycles* **27**, 882–893 (2013).
14. Yu, J. M., Elderfield, H. & Piotrowski, A. Seawater carbonate ion-$\delta^{13}C$ systematics and application to glacial–interglacial North Atlantic ocean circulation. *Earth Planet. Sci. Lett.* **271**, 209–220 (2008).
15. Zeebe, R. E. & Wolf-Gladrow, D. A. in *CO_2 in Seawater: Equilibrium, Kinetics, Isotopes* (ed. Halpern, D.) (Elsevier, 2001).
16. Key, R. M. *et al*. A global ocean carbon climatology: results from global data analysis project (GLODAP). *Glob. Biogeochem. Cycles* **18**, GB4031 (2004).
17. Broecker, W., Yu, J. & Putnam, A. E. Two contributors to the glacial CO_2 decline. *Earth Planet. Sci. Lett.* **429**, 191–196 (2015).
18. Raitzsch, M., Hathorne, E. C., Kuhnert, H., Groeneveld, J. & Bickert, T. Modern and late Pleistocene B/Ca ratios of the benthic foraminifer Planulina wuellerstorfi determined with laser ablation ICP-MS. *Geology* **39**, 1039–1042 (2011).
19. Yu, J. M. & Elderfield, H. Benthic foraminiferal B/Ca ratios reflect deep water carbonate saturation state. *Earth Planet. Sci. Lett.* **258**, 73–86 (2007).
20. Lisiecki, L. E. & Raymo, M. E. A Pliocene–Pleistocene stack of 57 globally distributed benthic $\delta^{18}O$ records. *Paleoceanography* **20**, PA1003 (2005).
21. Yu, J. *et al*. Deep South Atlantic carbonate chemistry and increased interocean deep water exchange during last deglaciation. *Quat. Sci. Rev.* **90**, 80–89 (2014).
22. Repschlager, J., Weinelt, M., Andersen, N., Garbe-Schonberg, D. & Schneider, R. Northern source for Deglacial and Holocene deepwater composition changes in the Eastern North Atlantic Basin. *Earth Planet. Sci. Lett.* **425**, 256–267 (2015).
23. Elderfield, H. *et al*. Evolution of ocean temperature and ice volume through the mid-pleistocene climate transition. *Science* **337**, 704–709 (2012).
24. Hodell, D. A., Charles, C. D. & Sierro, F. J. Late Pleistocene evolution of the ocean's carbonate system. *Earth Planet. Sci. Lett.* **192**, 109–124 (2001).
25. Oliver, K. I. C. *et al*. A synthesis of marine sediment core delta C-13 data over the last 150000 years. *Clim. Past* **6**, 645–673 (2010).
26. Le, J. & Shackleton, N. J. Carbonate dissolution fluctuations in the Western equatorial Pacific during the late Quaternary. *Paleoceanography* **7**, 21–42 (1992).
27. Howard, W. R. & Prell, W. L. Late quaternary $CaCO_3$ production and preservation in the Southern Ocean—Implications for oceanic and atmospheric carbon cycling. *Paleoceanography* **9**, 453–482 (1994).
28. Lyle, M. *et al*. in *Proceedings of the Ocean Drilling Program, Scientific Results* (eds Lyle, M., Koizumi, I., Richter, C. & Moore, T. C.) 163–182 (2000).
29. Ridgwell, A. J., Watson, A. J., Maslin, M. A. & Kaplan, J. O. Implications of coral reef buildup for the controls on atmospheric CO_2 since the last glacial maximum. *Paleoceanography* **18**, 1083 (2003).
30. Lea, D. & Boyle, E. Barium content of benthic foraminifera controlled by bottom–water composition. *Nature* **338**, 751–753 (1989).
31. Toggweiler, J. R. Origin of the 100,000-year timescale in Antarctic temperatures and atmospheric CO_2. *Paleoceanography* **23**, PA2211 (2008).
32. Broecker, W. S. & Peng, T. H. The role of $CaCO_3$ compensation in the glacial to interglacial atmospheric CO_2 change. *Glob. Biogeochem. Cycles* **1**, 15–29 (1987).
33. Emerson, S. & Archer, D. Glacial carbonate dissolution cycles and atmospheric p_{CO_2}: a view from the ocean bottom. *Paleoceanography* **7**, 319–331 (1992).
34. Marchitto, T. M., Lynch-Stieglitz, J. & Hemming, S. R. Deep Pacific $CaCO_3$ compensation and glacial–interglacial atmospheric CO_2. *Earth Planet. Sci. Lett.* **231**, 317–336 (2005).
35. Anderson, R. F., Fleisher, M. Q., Lao, Y. & Winckler, G. Modern $CaCO_3$ preservation in equatorial Pacific sediments in the context of late-Pleistocene glacial cycles. *Mar. Chem.* **111**, 30–46 (2008).
36. Yu, J. *et al*. Responses of the deep ocean carbonate system to carbon reorganization during the Last Glacial–interglacial cycle. *Quat. Sci. Rev.* **76**, 39–52 (2013).
37. Boyle, E. The role of vertical chemical fractionation in controlling late Quaternary atmospheric carbon dioxide. *J. Geophys. Res.* **93**, 15701–15714 (1988).
38. Gibbs, M. T. & Kump, L. R. Global chemical erosion during the last glacial maximum and the present: sensitivity to changes in lithology and hydrology. *Paleoceanography* **9**, 529–543 (1994).
39. Bohm, E. *et al*. Strong and deep Atlantic meridional overturning circulation during the last glacial cycle. *Nature* **517**, 73–76 (2015).
40. Ferrari, R. *et al*. Antarctic sea ice control on ocean circulation in present and glacial climates. *Proc. Natl Acad. Sci. USA* **111**, 8753–8758 (2014).
41. Ninnemann, U. S. & Charles, C. D. Changes in the mode of Southern Ocean circulation over the last glacial cycle revealed by foraminiferal stable isotopic variability. *Earth Planet. Sci. Lett.* **201**, 383–396 (2002).
42. Lynch-Stieglitz, J., Stocker, T. F., Broecker, W. & Fairbanks, R. G. The influence of air-sea exchange on the isotopic composition of oceanic carbon: observations and modeling. *Glob. Biogeochem. Cycles* **9**, 653–665 (1995).
43. Williams, R. G. & Follows, M. J. *Ocean Dynamics and the Carbon Cycle: Principals and Mechanisms* (Cambridge Univ. Press, 2011).

44. Menviel, L., England, M. H., Meissner, K. J., Mouchet, A. & Yu, J. Atlantic-Pacific seesaw and its role in outgassing CO_2 during Heinrich events. *Paleoceanography* **29**, 58–70 (2014).
45. Menviel, L., Joos, F. & Ritz, S. P. Simulating atmospheric CO_2, ^{13}C and the marine carbon cycle during the Last Glacial/Interglacial cycle: possible role for a deepening of the mean remineralization depth and an increase in the oceanic nutrient inventory. *Quat. Sci. Rev.* **56**, 46–68 (2012).
46. Menviel, L., Spence, P. & England, M. H. Contribution of enhanced Antarctic Bottom Water formation to Antarctic warm events and millennial-scale atmospheric CO_2 increase. *Earth Planet. Sci. Lett.* **413**, 37–50 (2015).
47. Schlitzer, R. *Ocean Data View* (2006); https://odv.awi.de

Acknowledgements

We thank J. McManus, D. Sigman and B. Anderson for insightful and constructive discussions and comments, and L. Kinsley and L. Rodriguez-Sanz for laboratory assistance. This work is supported by ARC Discovery Project (DP140101393) and Future Fellowship (FT140100993) to J.Y., CAS/SAFEA International Partnership Program for Creative Research Teams to J.Y. and Z.D.J., DECRA (DE150100107) to L.M., UK NERC grant NE/J008133/1 to S.B., and by Australian Laureate Fellowship (FL120100050) to E.J.R. Core materials were kindly provided by LDEO (N. Anest), NOC (G. Rothwell), GEREGE (N. Thouveny), and WHOI (E. Roosen/D. Oppo) core repositories. Model experiments were performed on a computational cluster owned by the Faculty of Science of the University of New South Wales as well as on a cluster from the NCI National Facility at the Australian National University.

Author contributions

J.Y. designed and performed the research and wrote the paper; L.M. carried out modelling; Z.D.J./F.Z. picked foram shells; D.J.R.T./S.B. and Y.D./P.C. generated data for MD95-2039 and EW9209-2JPC/RC16-59, respectively; G.M./E.J.R. conducted MC simulation; all authors contributed to improving the manuscript.

Additional information

Supplementary information is available in the online version of the paper. Reprints and permissions information is available online at www.nature.com/reprints. Correspondence and requests for materials should be addressed to J.Y.

Competing financial interests

The authors declare no competing financial interests.

Methods

Deep-water $[CO_3^{2-}]$ versus ALK–DIC. Owing to numerous equations and dissociation constants involved in the seawater carbonate system[15], we use the Global Ocean Data Analysis Project (GLODAP) data set[16] and model outputs from LOVECLIM and the UVic ESCM (refs 48–50) to explore the relationship between deep-water $[CO_3^{2-}]$ and ALK–DIC. For the GLODAP data set, the anthropogenic CO_2 contribution was subtracted from the measured DIC to obtain the pre-industrial values. Here we consider the deep Atlantic data (>2.5 km, 70° S–70° N, 15° E–65° W) from the GLODAP and model outputs. CO_2 system calculations are detailed in the Supplementary Information.

Core materials, analytical methods, and age model. We carried out new measurements on epibenthic (a habitat above the sediment–water interface) foraminiferal species *C. wuellerstorfi* from 7 cores. After sediment processing, benthic foraminiferal shells were picked, cleaned, and measured for $\delta^{18}O$, $\delta^{13}C$, and B/Ca following previous methods[51–54] (Supplementary Information). The analytical error in B/Ca is $\sim\pm 2.5\%$ ($\pm 3\,\mu mol\,mol^{-1}$), and $\sim 0.08‰$ in both $\delta^{18}O$ and $\delta^{13}C$. Age models for sediment cores are based on comparisons of benthic $\delta^{18}O$ with the LR04 stack curve[20] (Supplementary Table 2 and Supplementary Fig. 4). By using one target curve for tuning, we minimize potential relative age offsets between cores.

Deep-water $[CO_3^{2-}]$ reconstruction from benthic B/Ca. To convert *C. wuellerstorfi* B/Ca into deep-water $[CO_3^{2-}]$, we use $[CO_3^{2-}]_{downcore} = [CO_3^{2-}]_{Preindustrial} + \Delta B/Ca_{downcore\text{-}coretop}/1.14$, where $[CO_3^{2-}]_{Preindustrial}$ is estimated using the GLODAP data set[16] (Supplementary Table 1), $\Delta B/Ca_{downcore\text{-}coretop}$ represents the deviation of B/Ca of down-core samples from the core-top value, and the term 1.14 denotes the sensitivity of *C. wuellerstorfi* B/Ca to deep-water carbonate saturation state based on core-top calibration[18,19,36,55,56]. We quote an uncertainty of $\pm 5\,\mu mol\,kg^{-1}$ in $[CO_3^{2-}]$, based on the error derived from the global core-top calibration samples[19,36]. See Supplementary Information for details.

Data. All new data presented in this study are given in the Supplementary Tables.

Code availability. We have opted not to make the computer codes associated with this paper available because they are based on simple Ocean Data View[47] and CO_2sys (ref. 57) data analyses and established statistics[3,58].

References

48. Weaver, A. J. *et al*. The UVic earth system climate model: model description, climatology, and applications to past, present and future climates. *Atmos.-Ocean* **39**, 361–428 (2001).
49. Menviel, L., Timmermann, A., Mouchet, A. & Timm, O. Meridional reorganizations of marine and terrestrial productivity during Heinrich events. *Paleoceanography* **23**, A1203 (2008).
50. Meissner, K. J., Schmittner, A., Weaver, A. J. & Adkins, J. The ventilation of the North Atlantic Ocean during the Last Glacial Maximum: a comparison between simulated and observed radiocarbon ages. *Paleoceanography* **18**, 1023 (2003).
51. Yu, J. M., Elderfield, H., Greaves, M. & Day, J. Preferential dissolution of benthic foraminiferal calcite during laboratory reductive cleaning. *Geochem. Geophys. Geosyst.* **8**, Q06016 (2007).
52. Barker, S., Greaves, M. & Elderfield, H. A study of cleaning procedures used for foraminiferal Mg/Ca paleothermometry. *Geochem. Geophys. Geosyst.* **4**, 8407 (2003).
53. Yu, J. M., Day, J., Greaves, M. & Elderfield, H. Determination of multiple element/calcium ratios in foraminiferal calcite by quadrupole ICP-MS. *Geochem. Geophys. Geosyst.* **6**, Q08P01 (2005).
54. Boyle, E. & Keigwin, L. D. Comparison of Atlantic and Pacific paleochemical records for the last 215,000 years: changes in deep ocean circulation and chemical inventories. *Earth Planet. Sci. Lett.* **76**, 135–150 (1985).
55. Yu, J., Anderson, R. F. & Rohling, E. J. Deep ocean carbonate chemistry and glacial–interglacial atmospheric CO_2 changes. *Oceanography* **27**, 16–25 (2014).
56. Brown, R. E., Anderson, L. D., Thomas, E. & Zachos, J. C. A core-top calibration of B/Ca in the benthic foraminifers Nuttallides umbonifera and Oridorsalis umbonatus: a proxy for Cenozoic bottom water carbonate saturation. *Earth Planet. Sci. Lett.* **310**, 360–368 (2011).
57. Pelletier, G., Lewis, E. & Wallace, D. *A Calculator for the CO_2 System in Seawater for Microsoft Excel/VBA* (Washington State Department of Ecology, Olympia, WA, Brookhaven National Laboratory, Upton, NY, 2005).
58. Rohling, E. J. *et al*. Sea-level and deep-sea-temperature variability over the past 5.3 million years. *Nature* **508**, 477–482 (2014).